Application of Finite-Strip Method to Cylindrical Shells Partially Buried in Elastic Foundation

Hokkaido University	Student Member	○ Haryadi Gunawan
Koken Engineering Co. Ltd	Member	Hidehiro Kyoda
Hokkaido University	Fellow Member	Takashi Mikami
Hokkaido University	Member	Shunji Kanie
Hokkaido University	Member	Motohiro Sato

1. Introduction

In practical application, circular cylindrical shells are frequently used and may be subjected to various kind of loading such as pressure loading in the closed cylindrical vessels, gravity load, water pressure and etc. It is common in the field of tunneling and pipelining that somehow the cylindrical shells are placed on the soil as a foundation. Knowing the basic soil structure interaction of the considered problem is necessary to assess the behavior of such structures properly. Partially distributed elastic foundation of the cylindrical shell has been modeled by Amabili [1] but only the radial displacement was being adopted.

The purpose of this paper is to introduce a method to analyze the cylindrical shells on partially distributed elastic foundation along the circumferential direction by taking into account the end conditions and other displacement parameters as been described above, subjected to any kind of loadings.

2. Model

2.1. General

The cylindrical shells are modeled by using isotropic thin elastic cylindrical shell element. The considered problem is shown in figure 1. In this study, local stability of the cylindrical shell is assured and satisfied for the whole analysis. The stresses developed within the shell element are considered relatively small enough to prevent the local instability such as buckling of the shell.

The soil as foundation is modeled by elastic spring which is connected to shell in radial direction, but it is possible by using the same method described here to include the axial and circumferential spring. For the sake of simplicity only radial spring is considered and distributed at limited arc along the circumferential direction as shown in Fig.1.

In the present study, since based on finite strip method, which implied the generalization of the strip in one direction, that is the circumferential, and then the foundation distribution function has to be made general along this direction.

Generalized strip and reference axis used in this paper are shown in Fig.2. In order to do so, Fourier series is used to

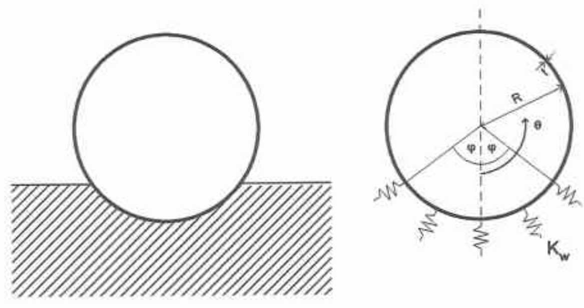

Fig.1. Generalized model

define the radial elastic spring distribution as shown in (1), in which K_w is the radial spring constant, and an example for the foundation distribution obtained by Fourier series for $\varphi = 60^\circ$ is given in Fig.3.

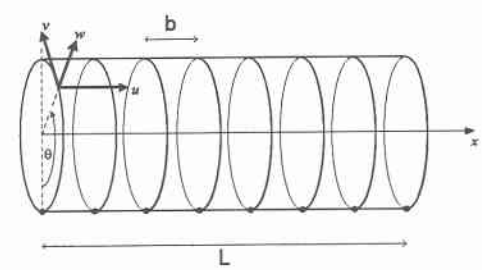

Fig.2. Strip and reference direction

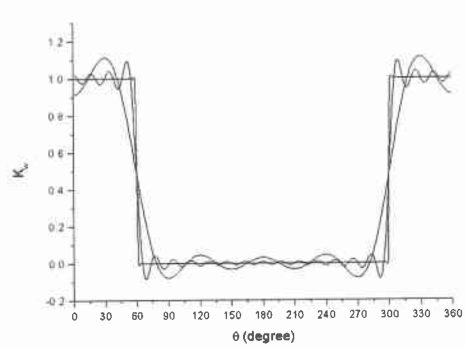

Fig.3. Foundation distribution

$$\kappa(\theta) = \frac{K_w}{\pi}\left\{\varphi + \sum_{\ell=1}^{\infty}\left[\frac{2\sin(\ell\theta)}{\ell}\cos(\ell\theta)\right]\right\} \tag{1}$$

2.2. Finite Strip Formulation

In finite strip method, the displacement function is defined by simple polynomial in one direction and continuous differentiable function in other direction. As for this problem the displacement function is so been chosen a priori to satisfied the problem's boundary condition. The axial, circumferential, radial and radial slope displacement function are shown as u, v, w, and β respectively in (2) for an axisymmetrical problem. After arrangement, the overall displacement can be defined as given in (3), which is lead to the general form as in finite element method. For axial and circumferential displacement, simple linear function is used, but for radial displacement cubic polynomial in longitudinal direction is used.

$$\begin{aligned} u(x,\theta) &= \sum_{m=0}^{M} f_m^u(x)\cos(m\theta) = \sum_{m=0}^{M}\left[\mathbf{N}^u\right]_m \left\{\boldsymbol{\delta}_e^u\right\}_m \\ v(x,\theta) &= \sum_{m=0}^{M} f_m^v(x)\sin(m\theta) = \sum_{m=0}^{M}\left[\mathbf{N}^v\right]_m \left\{\boldsymbol{\delta}_e^v\right\}_m \\ w(x,\theta) &= \sum_{m=0}^{M} f_m^w(x)\cos(m\theta) = \sum_{m=0}^{M}\left[\mathbf{N}^w\right]_m \left\{\boldsymbol{\delta}_e^w\right\}_m \\ \beta(x,\theta) &= \sum_{m=0}^{M} f_m^\beta(x)\cos(m\theta) = \sum_{m=0}^{M}\left[\mathbf{N}^\beta\right]_m \left\{\boldsymbol{\delta}_e^\beta\right\}_m \end{aligned} \tag{2}$$

$$\{\boldsymbol{\delta}\} = [\mathbf{N}]\{\boldsymbol{\delta}_e\} \tag{3}$$

The curvature changes and strain matrix of the elastic cylindrical shell is shown in (4) and the final arrangement is given in (5).

$$\{\boldsymbol{\varepsilon}\} = \begin{Bmatrix} \varepsilon_x \\ \varepsilon_\theta \\ \varepsilon_{x\theta} \\ \chi_x \\ \chi_\theta \\ \chi_{x\theta} \end{Bmatrix} = \begin{Bmatrix} \dfrac{\partial u}{\partial x} \\ \dfrac{1}{R}\dfrac{\partial v}{\partial \theta} + \dfrac{w}{R} \\ \dfrac{1}{R}\dfrac{\partial u}{\partial \theta} + \dfrac{\partial v}{\partial x} \\ -\dfrac{\partial^2 w}{\partial x^2} \\ -\dfrac{1}{R^2}\dfrac{\partial^2 w}{\partial \theta^2} + \dfrac{1}{R^2}\dfrac{\partial v}{\partial \theta} \\ 2\left(-\dfrac{1}{R}\dfrac{\partial^2 w}{\partial x \partial \theta} + \dfrac{1}{R}\dfrac{\partial v}{\partial x}\right) \end{Bmatrix} \tag{4}$$

$$\{\boldsymbol{\varepsilon}\} = \sum_{m=0}^{M}[\mathbf{B}]_m\{\boldsymbol{\delta}_e\}_m = [\mathbf{B}]\{\boldsymbol{\delta}_e\} \tag{5}$$

As soon as the strain matrix is known then the formation of the stiffness matrix of the cylindrical shell can be obtain readily by using the well known relation shown in (6), in which **D** matrix is elasticity matrix.

$$[\mathbf{K_S}] = \int_V [\mathbf{B}]^{\mathrm{T}}[\mathbf{D}][\mathbf{B}]\,\mathrm{d}V \tag{6}$$

Since the **B** matrix is involving the trigonometric and also polynomial term, which can be integrated over the volume numerically, but in this study, the stiffness matrix of the shell is derived exactly by observing the nature of integrals developed in each element of the matrix. The foundation stiffness matrix derived by using (7) and (8) in which the only element in $\mathbf{k_f}$ is corresponding with the spring distribution in radial direction.

$$[\mathbf{K_F}] = \int_A [\mathbf{N}]^{\mathrm{T}}[\mathbf{k_f}][\mathbf{N}]\,\mathrm{d}A \tag{7}$$

$$[\mathbf{k_f}] = \begin{bmatrix} 0 & 0 & 0 & 0 \\ 0 & 0 & 0 & 0 \\ 0 & 0 & \kappa(\theta) & 0 \\ 0 & 0 & 0 & 0 \end{bmatrix} \tag{8}$$

N matrix also contains the trigonometric term in m and n, again more sophisticate observation to the nature of integrals had to be performed in order to derive the foundation stiffness matrix without any loss of precisions due to numerical integration. Another problem is the combination of m, n (harmonic term correspond to displacement function) and ℓ (harmonic term correspond to foundation distribution function) that after some fundamental trigonometric transformations will form typical integrals shown in (9).

$$\begin{aligned} &\int_0^{2\pi}\cos\left((m+n)\theta\right)\cos(\ell\theta)\,\mathrm{d}\theta \\ &\int_0^{2\pi}\cos\left((m-n)\theta\right)\cos(\ell\theta)\,\mathrm{d}\theta \end{aligned} \tag{9}$$

These integrals have a value that is π only if $m+n=\ell$ or $m-n=\ell$, whereas the other combinations give zero to the integrals. Knowing those facts, ℓ term can be taken infinity, and as a result, the ℓ term always provide sufficient number to give a value to the integrals developed in the matrix under any combinations of m and n.

Furthermore, the foundation stiffness matrix will take a full matrix form that implied the coupling phenomenon of the term m and n, which is different from the form of shell stiffness matrix.

The load matrix can be derived by the similar way as for the stiffness matrix, since basically just generalized the function of load in circumferential direction by the mean of Fourier series, and the equivalent nodal load can be obtained without any difficulties. Some load cases have been analyzed to show the capability of the method described here for any kind of loadings, such as internal pressure load, gravity load, hydrostatic pressure, and enclosed liquid pressure load as shown in Fig.4.

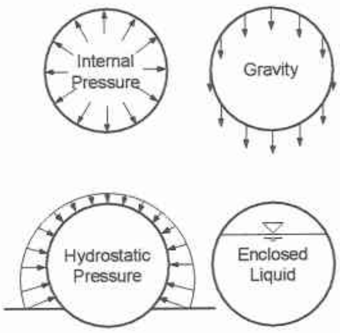

Fig.4. Load cases

The assemblage of the whole equation and application of boundary condition are the same as in finite element method which is shown in (10).

$$\left[\left[\mathbf{K_S}\right]+\left[\mathbf{K_F}\right]\right]\{\delta_e\}=\{\mathbf{F}\} \tag{10}$$

3. Numerical Result

3.1. Convergence

Numerical example presented here is dealt with the most common load that is gravity load, with both clamped ends condition, $R/L = 0.025$, $t/L = 0.00075$, $k\,L/E = 9.0 \times 10^{-4}$, $q/E = 5.0 \times 10^{-8}$, $\varphi = 60^{\circ}$, $\nu = 0.30$. Convergence rate are given in Fig.4, 5, 6 for displacement, normal, and moment at centerline section for total number of harmonic $M = 5$. Total deformation of analyzed middle section is shown in Fig.7. The axial, shear, and twisting moment at middle section is zero and the result assess this value by very small value nearly equal to zero.

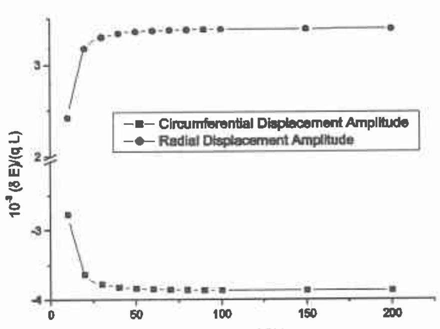

Fig.5. Convergence rate of displacements

The convergence rate is influenced not only by the number of strip but also by number of harmonic term. The number of term which is needed for convergence is differed for each problem. Problem with relatively large *R/t* on very stiff foundation as a base, the convergence can be obtained by increasing the number of term *m*. The only reason for this is the sudden changes in displacements at near the border between last spring and air.

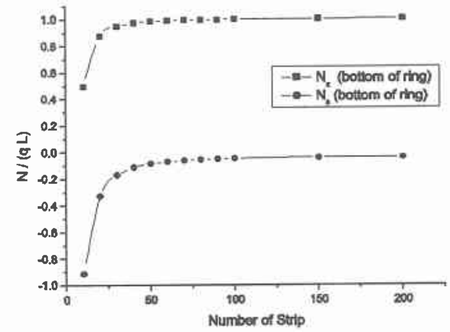

Fig.6. Convergence rate of internal forces

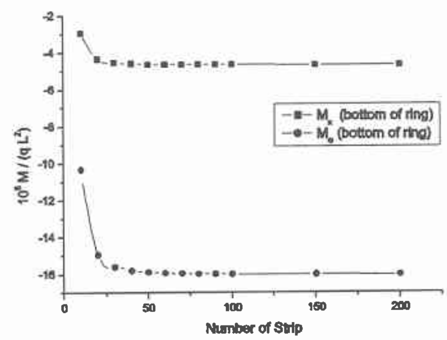

Fig.7. Convergence rate of internal moment

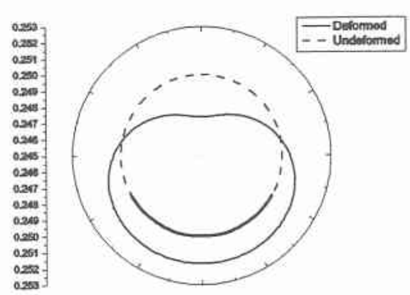

Fig.8. Total deformation of middle section

3.2. Parameter Relationships

The same problem with both ends clamped is considered in this part by analyzing the middle section.

Radial displacement at bottom of ring section is represented by total radial amplitude exactly, and the circumferential displacement at side of the ring is represented by total circumferential amplitude approximately. For considered thick shells, the radial displacement at bottom or top of the ring and circumferential displacement at side of the ring is almost the same because of high sectional rigidity.

The displacement characteristics are influenced by the confinement effect of foundation surrounding the shell and can be seen in Fig.9-13.

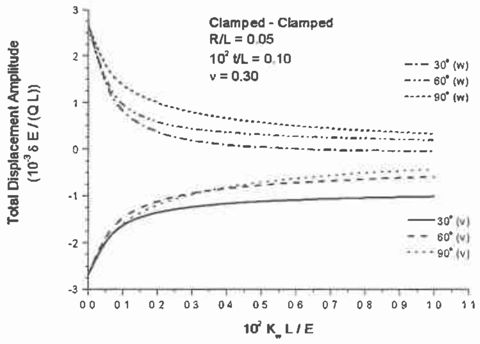

Fig.9. Variation of circumferential and radial total amplitude with foundation stiffness parameter

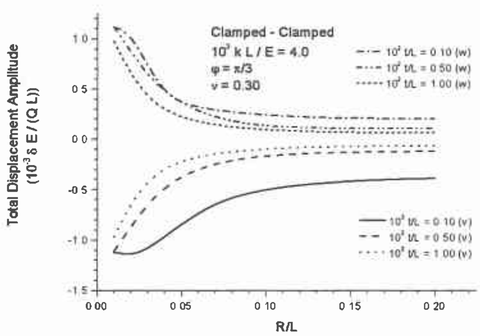

Fig.10. Variation of circumferential and radial total amplitude with radius of shell

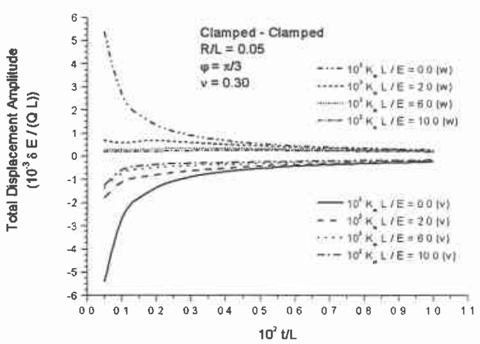

Fig.11. Variation of circumferential and radial total amplitude with thickness of shell

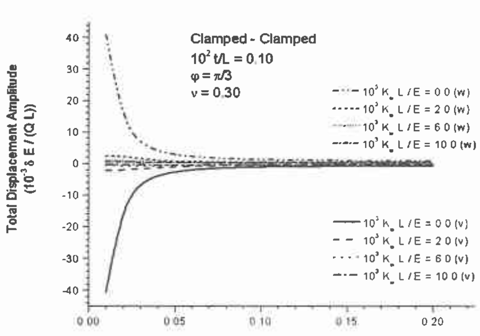

Fig.12. Variation of circumferential and radial total amplitude with radius of shell

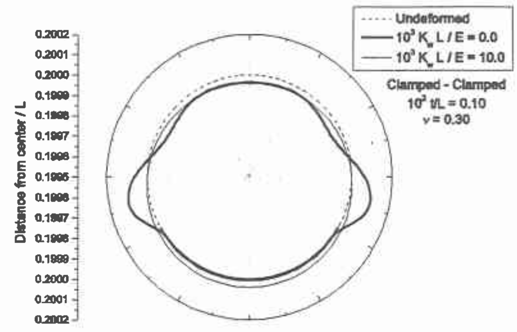

Fig.13. Sectional deformation

4. Conclusion

The present method is suitable and efficient for analyzing the considered problem with good geometrical representation to the actual structure condition. A word of attention should be added regarding the convergence of the result which is indirectly influenced by geometrical parameter of shell and stiffness of foundation. The method is capable to assess the sectional deformation for the whole structure.

References

1) Amabili, Marco. and Dalpiaz, Giorgio.: Free Vibration of Cylindrical Shells with Non-Axisymetric Mass Distribution on Elastic Bed, Meccanica, Vol 32, pp.71-84, 1997.
2) Cheung, Y.K.: Finite Strip Method in Structural Analysis, Pergamon Press, 1st Edition, 1976.
3) Timoshenko, Stephen.P. and Krieger.: Theory of Plates and Shells, McGraw-Hill Kogakusha, ltd, 2nd Edition, 1959.